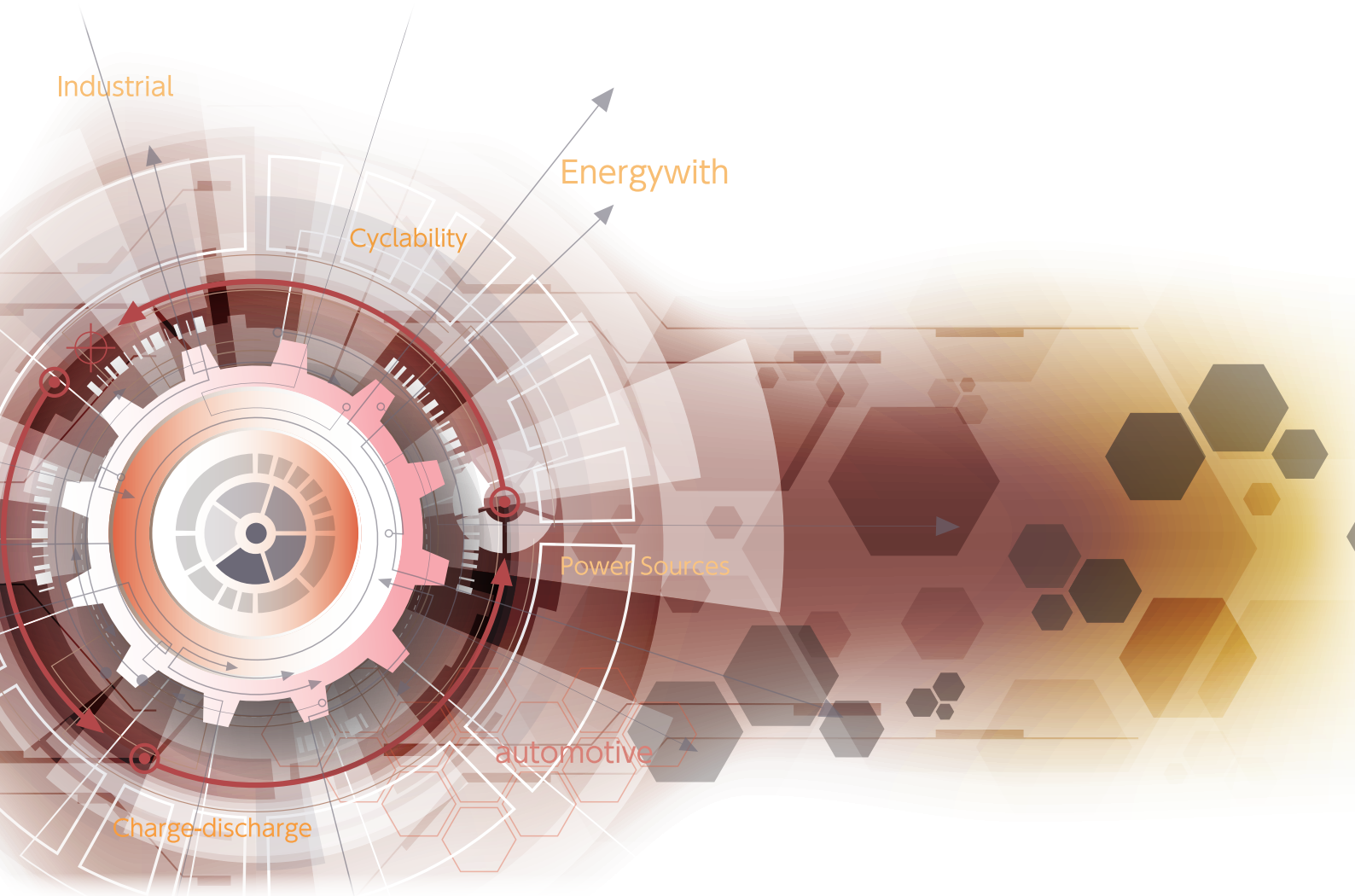


# Energywith Technical Report

No. 02 (May 2024)



# Energywith Technical Report

No. 02 (May 2024)



## Commentary

- EW Technical Report ..... 3  
Masato Yoshida

## Contribution

- Development of Dual-Ion Battery Using Graphene-like Graphite ..... 5  
Yoshiaki Matsuo

## Report

- Analysis of operating data of LL batteries at wind power plants  
by using exploratory data analysis and other analyses for their life prediciton ..... 10  
Kei Hasegawa . Daisuke Hosaka . Toshio Shibahara . Noriyuki Tamura
- Development of algorithm for image inspection of COS (Cast On Strap) process ..... 14  
Masahide Ohno
- A new DIN-Type Traction Battery ..... 17  
Warakorn Suriyatun . Pratan Pongphongpoon . Chakkapan Sangkaew . Muneyoshi Noda
- "withBMS", the battery monitoring service of  
lead acid batteries for electric folkklifts ..... 21  
Akihiko Kudou . Koji Hayata



President and Chief  
Executive Officer

**Masato Yoshida**

# Energywith Technical Report

Two years have passed since Energywith (EW) was founded. We continue to drive our business operations, guided by the corporate philosophy established at EW's inception: "ENERGYWITH , adds new wisdom to energy storage and focuses on quality to provide people with reliability and safety as a trusted energy storage solution company". We prioritize "Performance", "Quality" and "Sales Capability" and strive daily to improve these areas with all employees. This technical report shows our achievements in Performance and Quality.

Three out of four of the papers submitted to EW focus on technology development through digital transformation (DX). A decade ago, I attended a technology presentation by a metal materials manufacturer. The subtopic was technology development using computer aided engineering (CAE), which involves simulating, calculating and analyzing various physical phenomena related to products on computers, primarily in the design and development of industrial products. At this presentation, I was amazed to learn that large automotive parts had been designed and prototyped on a computer without making an actual prototype and that their durability had been simulated to obtain customer certification. In the world of chemical materials, it had just become possible to estimate the optimum material composition using historical data, which was a real game-changer for me. The President concluded the presentation by saying, "Technology development exists for manufacturing and the President will actively promote new technological innovations." When the EW group was established, analog technology development was still mainstream, and knowledge was primarily accumulated within individuals. As stated above, we began with the theme of "quality" improvement, assisted by external experts utilizing statistical analysis tools, inspired by the words, "the president will actively drive new technological innovation." To turn a large gear, a significant amount of force is initially required; however, once the gear starts turning, it accelerates. The progress of EW's engineers in utilizing DX mirrors this analogy, as reflected in the content of this report.

While we are still on this journey, leveraging digital transformation (DX) is essential to transforming from a company that sells storage batteries to one that offers energy storage solutions and provides knowledge about storage batteries as value. We want to continue evolving.



The "Development of algorithm for image inspection of COS (Cast On Strap) process" is crucial for quality improvement using DX. This is a common issue across EW group sites, and we plan to develop it within the group. The "withBMS", the battery monitoring service of lead acid batteries for electric forklifts" detects and monitors various conditions of storage batteries when operated by clients, providing them with detailed insights. This service visualizes the operation status of storage batteries (water supply/charging) and offers improvement proposals to clients. This is the kind of technology development essential for transforming from a battery-selling business to an energy storage solution business. The "Analysis of operational data of LL batteries at wind power plants by using exploratory data analysis and other analyses for their life prediction" identified factors affecting battery lifespan using big data accumulated from customers and machine learning. This technology is expected to evolve into energy storage solutions that monitor system degradation in real time, meeting customer needs while preserving battery life.

As development of new products, report details titled "A new DIN-Type Traction Battery" are posted by a group company in Thailand, TES (Thai Energy Storage Technology PLC.). DIN standard (set by the German Institute for Standardization) storage batteries are expanding in South Asia. TES has successfully launched this new product on the market utilizing JIS standard storage battery technology possessed by EW group. The global share of DIN standard is 60%. We hope that this technology will contribute to business expansion of TES.

In this volume, Professor Matsuo from Graduate School of Engineering, University of Hyogo contributed about research content of new storage batteries with the title "Development of Dual-Ion Battery Using Graphene-like Graphite". Graphite is a material that is used as negative electrode materials for lithium-ion batteries. This is a research of breakthrough technology for creating a structure that doesn't exist in graphite to use carbon materials for both positive and negative electrodes by devising graphene processing conditions. This Graphene-like graphite can be used for not only negative electrode but also positive electrode. As professor has pointed out, low resource risk is an important factor. Furthermore, the carbon material is also attractive because it is lightweight and inexpensive. We would like to thank Professor Matsui for contributing his valuable research content to EW's Technical Report. EW will also continue to develop new storage batteries that will contribute to recycling society and low carbon society with the support of external parties including Professor Matsuo. We will do our best to help you understand the direction EW is aiming for through this Technical Report. Thank you for your continued guidance.

# Development of Dual-Ion Battery Using Graphene-like Graphite

Yoshiaki Matsuo  
University of Hyogo

## 1 Abstract

The thermal treatment of graphite oxide provides carbon materials consisting of regularly stacked graphenes possessing oxygen atoms and nano-pores. We named these materials as graphene-like graphite (GLG) and used as the active materials of dual-ion batteries (DIB). The reversible capacity of GLG as the cathode of DIB reached  $147 \text{ mAh g}^{-1}$  with a low upper limit potential of 4.8 V vs  $\text{Li}^+/\text{Li}$ . The theoretical calculations indicated that it is ascribed to the newly emerged bands. The charge-discharge reactions of DIB using GLG as both anode and cathode successfully occurred when anode was precycled and  $66 \text{ mAh g}^{-1}$  of reversible capacity was achieved. At this moment, the energy density was calculated to be  $124 \text{ Wh kg}^{-1}$ , however, further investigation would improve the performance and more than  $300 \text{ Wh kg}^{-1}$  of energy density would be expected.

## 2 Introduction

In recent years, the need to solve environmental problems such as global warming has become urgent. To do this, we need to transform our entire economic and social system, known as the Green Transformation (GX). One important transformation is the electrification of vehicles, which significantly reduces the use of fossil fuels. Although vehicle electrification is progressing rapidly, further acceleration will require the improvement of current liquid system lithium-ion batteries (LIBs) in electric vehicles and the development of next-generation batteries, including solid-state LIBs and other innovative storage batteries.

In addition, natural resource supply risks have increased, driving demand for low-cost materials with low raw material supply risks. To meet this demand, we need storage batteries that combine high energy density, durability, longevity and safety with low resource risk and minimal environmental impact. METI's Research and Development Initiative for Scientific Innovation of New Generation Batteries 3 (RISING3) is promoting the development of zinc negative electrode batteries and fluoride shuttle batteries. Meanwhile, JST's Green Technologies of Excellence (GteX) is supporting the development of sodium-ion and magnesium batteries.

We are exploring the use of carbon materials, produced by heat treating graphite oxide (also known as graphene oxide), for LIBs. Carbon has a relatively low resource risk and is lightweight and conductive, making it a promising active material for these innovative storage batteries. This article presents the development of dual-ion batteries using this carbon material, called "graphene-like graphite" (GLG).

## 3 Regarding GLG

Graphite oxide (GO) is a type of covalent graphite intercalation compound that has hydroxy and epoxy groups introduced on the carbon layer surface. It was first synthesized in the 1850s. Since GO can be exfoliated to a single layer in solution, it has recently been actively researched as a precursor to graphene. The oxygen-containing functional groups in GO can be removed by vacuum treatment, heating under an inert atmosphere, or reacting with a reducing agent. During thermal reduction, rapid heating

causes the sample to expand, whereas slow heating produces a carbon material with oxygen and nanopores on the carbon layer surface, maintaining the same laminated structure as the original graphite. Although this synthesis of this material has long been carried out, we found that lithium intercalation/deintercalation behavior was unique<sup>1-3)</sup> when it was used as a lithium-ion battery negative electrode in 1998. Currently, this carbon is named GLG<sup>4)</sup> and we are considering using it not only for active material for the negative electrode of a lithium battery<sup>5-11)</sup>, but also for other power storage devices (sodium-ion batteries<sup>12, 13)</sup> dual-ion batteries<sup>14-16)</sup> fluoride shuttle batteries<sup>17)</sup> and zinc negative electrode batteries).

**Figure 1** shows the structural model of graphene-like graphite (GLG) that we propose<sup>4)</sup>, based on analysis using various spectroscopic methods and theoretical calculations. In GLG, oxygen is introduced in opposite positions in the form of C-O-C bonds. It is believed to exist as a lactone around nanopores measuring about 1-5 nm. Reduced graphene oxide (rGO), which is carbon obtained by reducing GO, is also widely studied. However, rGO layers tend to peel off, resulting in a large surface area in many cases. In contrast, GLG has a small surface area and retains almost the same morphology as graphite, making it easier to handle similarly to graphite. Elemental analysis of GLG shows that the oxygen content is about 10% at 300°C. This oxygen content decreases with increasing heat treatment temperature and is no longer detected above 1000°C. Additionally, the distance between carbon layers in GLG is 0.4 nm at 300°C. This distance decreases with higher heat treatment temperatures, becoming the same or smaller than that of graphite around 900°C, then slightly increasing again.

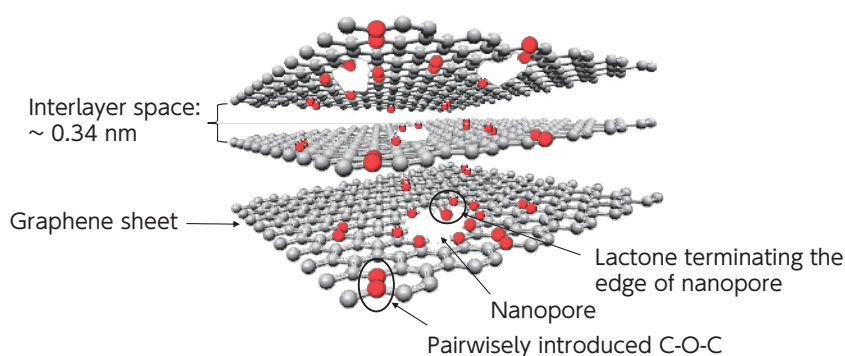


Figure 1. A structure model of graphene-like graphite Reproduced from Ref.4 Copyright The authors

## 4 Regarding dual-ion batteries

The dual-ion battery was developed in 1989 as a device that operates by storing anions and cations in the positive and negative electrodes respectively<sup>18, 19)</sup>. As graphite was often used as the active material for both poles, it also called dual carbon battery, however, various materials have been considered for both positive and negative electrodes in recent years. When using lithium-based electrolyte and graphite for both electrodes, insertion and extraction of lithium ions occurs at negative electrode in the same way as lithium-ion batteries. The saturated composition is  $\text{LiC}_6$  and the theoretical capacity is  $372 \text{ mAh g}^{-1}$ . Conversely, at the positive electrode, insertion and extraction of an anion occur. The saturated composition is estimated to be  $\text{C}_{20}\text{PF}_6^-$  in case of  $\text{PF}_6^-$  ion. In this case, the capacity is  $112 \text{ mAh g}^{-1}$ , which is smaller than the capacity of the positive electrode of an existing lithium-ion battery<sup>20)</sup>. In addition, to obtain this capacity, since a charging voltage of around 5 V vs  $\text{Li}^+/\text{Li}$  is required, the choice of electrolyte is also limited. Accordingly, a positive electrode with higher capacity that could be charged at a lower potential has been desired.

## 5 Dual-ion battery positive electrode characteristics of graphene-like graphite<sup>14)</sup>

**Figure 2** shows the charge-discharge curve of GLG synthesized at 700°C and that of graphite when performing constant current charging and discharging in 3M  $\text{LiPF}_6$ -ethyl methyl carbonate. With graphite, charging began around 4.7 V, reaching a capacity of  $50 \text{ mAh g}^{-1}$  when the upper limit potential was set to 4.8 V. In contrast, with GLG, charging started around 4.3 V and reached  $150 \text{ mAh g}^{-1}$ . During discharging, the voltage decreased linearly, and the discharge capacity at 2.0 V reached  $137 \text{ mAh g}^{-1}$ , approximately three times that of graphite. The initial coulombic efficiency was relatively high at 91%. X-ray diffraction measurements revealed structural changes during charging and discharging.  $\text{PF}_6^-$  ions were stored between the layers, forming a stage structure similar to graphite. It was found that  $\text{PF}_6^-$  ions were already inserted between all layers at 4.6 V with GLG, whereas with graphite at this potential,  $\text{PF}_6^-$  ions were inserted only between every other carbon layer. This difference explained the

significant capacity difference. During discharging, the structure was not completely restored even after discharging to 2.0 V, and a small amount of  $\text{PF}_6^-$  ions remained between the layers.

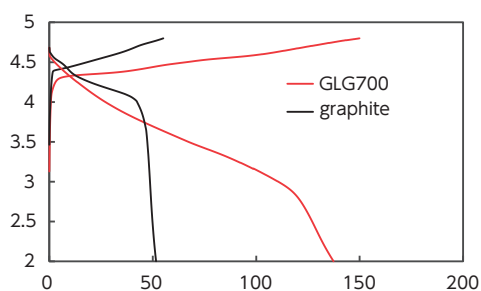


Figure 2. Charge-discharge curves of GLG700 and graphite electrodes. Reproduced from Ref.14 Copyright The authors

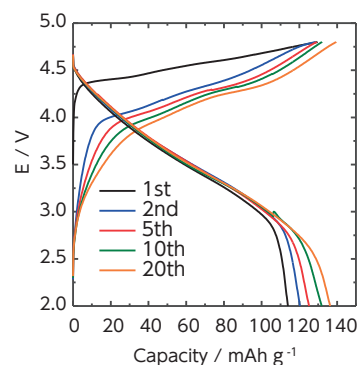


Figure 3. Charge-discharge curves of GLG700 electrode. Reproduced from Ref.14 Copyright The authors

**Figure 3** shows the cycle characteristics. As the charging potential gradually decreases with each cycle, the capacity below 2.5 V during discharge increased, reaching  $147 \text{ mAh g}^{-1}$  after 20 cycles. X-ray diffraction measurements indicated that the planar spacing of the carbon layers increased gradually after charging. This suggests that the battery could be charged more deeply with each cycle.

As stated above, GLG's oxygen content and the distance between carbon layers vary depending on the synthesis temperature and can also be altered by changing the synthesis method of GO. We synthesized GLG with various distances between carbon layers (0.332-0.377 nm) and O/C ratios (0.001-0.103) to measure charge-discharge performance. **Figure 4** shows the first cycle discharge capacity plotted against oxygen content. The capacity rapidly increased with rising oxygen content up to a point before it began to decrease.<sup>15)</sup>

Density functional theory calculations of the electronic states of various GLGs revealed a new state near the Fermi level that is not present in graphite. This indicates that the energy required to remove electrons from GLG is small, which makes anion insertion easier and increases capacity.<sup>21)</sup>

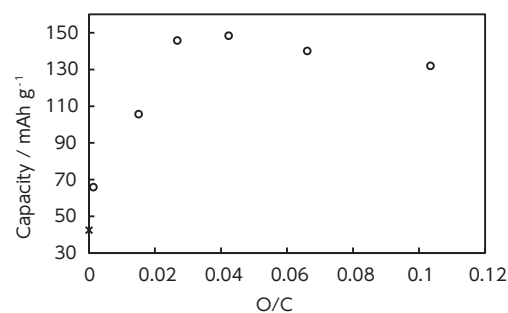


Figure 4. Relationships between capacity of GLG and O/C ratio. Reproduced with permission from Ref.15 Copyright 2022 John Wiley and Sons.

## 6 Characteristics of dual-ion battery using graphene-like graphite for both poles<sup>16</sup>

If GLG is used as a lithium-ion battery negative electrode, it exhibits greater capacity and better input/output characteristics than graphite and is less prone to metallic lithium deposition when charging rapidly. Accordingly, it has emerged as a highly safe material. GLG capacity varies depending on oxygen content and reaches  $670 \text{ mAh g}^{-1}$  for those with an oxygen content of about 10.5%, however, in this research, GLG obtained by processing at  $700^\circ\text{C}$  whose amount of oxygen was approximately 5% was used for both positive and negative electrodes.

**Figure 5** shows the charge-discharge curve when  $3\text{M LiPF}_6\text{-EMC}$  is used as the electrolyte. During charging, a short plateau with small voltage changes was observed around 2 V, followed by a similar plateau around 3.8 V. The charging capacity was  $58 \text{ mAh g}^{-1}$ . Conversely, during discharging, the voltage suddenly decreased from around 3 V, and the discharging capacity was small, at  $5 \text{ mAh g}^{-1}$ . At this time, the positive electrode potential was about 4.5 V, reaching the region where anion insertion occurs. In contrast, the negative electrode showed plateaus at 2.5 and 0.9 V, not reaching the lithium insertion potential. This indicates that some side reactions occurred on the negative electrode. When charging and discharging are performed with the negative electrode alone, there is no plateau around 2.5 V, suggesting that the products generated at the positive electrode move and react at the negative electrode. SEM observation confirmed deposits on the positive electrode surface, verifying this side reaction.

To address this, we formed a protective film on the negative electrode to suppress side reactions and performed full cell charging/discharging after precycling the negative electrode, as shown in **Figure 6**.

In addition, GLG generated at 300°C was used, which has a lower charging potential for the positive electrode. As a result, the plateau observed in the low voltage region during the initial charge was no longer present, allowing charging and discharging to proceed smoothly. The potential of each electrode, indicated by the dotted line, showed changes similar to those observed when evaluated with half-cells. When the upper limit voltage was set at 4.6 V, the discharge capacity reached 66 mAh g<sup>-1</sup> per weight of the positive electrode. Consequently, the energy density per electrode was 124 Wh kg<sup>-1</sup>, based on an average voltage of 2.5 V and the weight ratio of the positive and negative electrodes. Although this value is not large, the maximum capacities for the positive and negative electrodes were 150 and 670 mAh g<sup>-1</sup> respectively<sup>6,15</sup>. Therefore, with further improvements, we can expect the value to reach 300 Wh kg<sup>-1</sup>. These results indicate that dual carbon batteries using GLG for both electrodes are promising as a high safety, high input/output next generation battery.

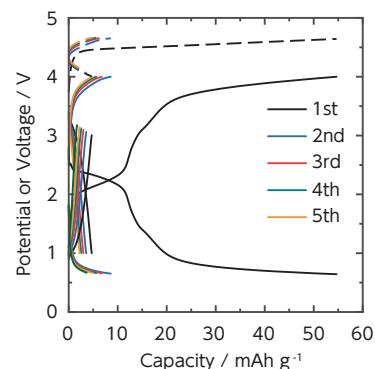


Figure 5. Charge-discharge curves of the full cell with lithium metal reference electrode in 3 mol dm<sup>-3</sup> LiPF<sub>6</sub>/EMC. The bold lines indicate voltage curves of full cell(cathode vs. anode). The dashed and thin lines indicate potential curves of cathode and anode vs. lithium metal reference electrode, respectively. The cathode/anode weight ratio was 3.3. The capacity is divided by the active material weight of the cathode. Reproduced from Ref.16 Copyright The authors

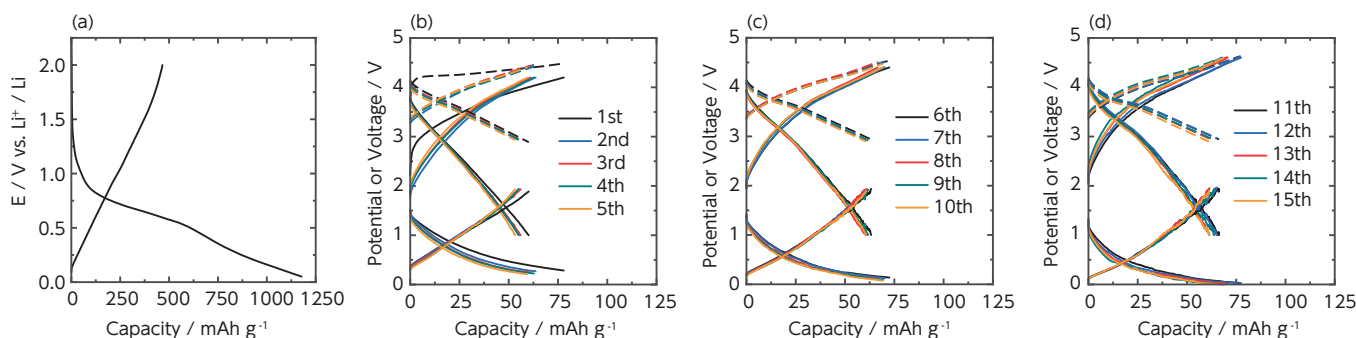


Figure 6. Charge-discharge curves of the full cell with lithium metal reference electrode in 3 mol dm<sup>-3</sup> LiFSA/EMC. The weight ratio of cathode and anode was 3.4.(a): Charge-discharge curves of GLG700 anode during precycling. (b), (c), and (d): Charge-discharge cycles of the full cell. The bold lines indicate voltage curves of full cell(cathode vs. anode). The dashed and thin lines indicate potential curves of cathode and anode vs. lithium metal reference electrode, respectively. Upper limit of cut-off voltage was set at 4.2V(b), 4.4V(c), and 4.6V(d) vs. Li<sup>+</sup>/Li. The capacities in(b), (c) and (d) are divided by the active material weight of the cathode. Reproduced from Ref. 16 Copyright The authors.

## 7 Conclusion

As stated above, GLG allows both cations and anions to insert and extract more easily than graphite, and in greater amounts, making it an excellent electrode material for dual-ion batteries. Although many issues remain to be resolved for practical application, such as reducing irreversible capacity and establishing industrial production methods for GLG, we are committed to addressing these challenges to contribute to the practical application of power storage devices using GLG. This Technical Report presents several energy storage solution technologies aimed at realizing Green Transformation (GX) and digital transformation (DX). As mentioned in Chapter 2, GLG can store various ions. We hope that next-generation batteries using GLG will become central to these energy storage solutions.

Results described in this paper were obtained through joint research with Assistant Professor Junichi Inamoto, Assistant Professor Akane Inoo and students from University of Hyogo. Furthermore, a part of this research was financially supported by Grant-in-Aid for Transformative Research Areas (A) (JP21H05237), which was greatly appreciated.

---

#### [References]

- 1) Y. Matsuo, et al : "Electrochemical intercalation of lithium into pyrolytic carbon from graphite oxide", *Electrochemistry*, vol. 66, pp. 1288-1290 (1998)
- 2) Y. Matsuo, et al : "Preparation, structure and electrochemical property of pyrolytic carbon from graphite oxide", *Carbon*, vol. 36, pp. 301-303 (1998)
- 3) Y. Matsuo, et al : "Pyrolytic carbon from graphite oxide as an anode of lithium-ion cells in 1M LiClO<sub>4</sub>-propylene carbonate solution", *Electrochemical and Solid State Letters*, vol.1 pp. 204-206 (1998)
- 4) Q. Cheng, et al : "Graphene-Like-Graphite as Fast-Chargeable and High-Capacity Anode Materials for Lithium Ion Batteries", *Sci. Rep.*, vol. 7, 14782 (2017)
- 5) Y. Matsuo, et al : "Electrochemical properties of nitrogen-doped carbons prepared by the thermal reduction of furfurylamine-intercalated graphite oxide", *Tanso*, vol. 281, pp. 2-7 (2018)
- 6) Y. Matsuo, et al : "Effect of oxygen contents in graphene like graphite anodes on their capacity for lithium ion battery", *J. Power Sources*, vol 396, pp. 134-140 (2018)
- 7) Y. Matsuo, et al : "Electrochemical intercalation behaviors of lithium ions into graphene like graphite", *J. Electrochem. Soc.*, vol 165, pp. A1-A6 (2018)
- 8) J. Inamoto, et al : "Effects of Pre-Lithiation on the Electrochemical Properties of Graphene-Like Graphite", *Electrochemistry*, vol 87, pp. 260-264 (2019)
- 9) S. Uchida : "Graphene-like graphite negative electrode rapidly chargeable at constant voltage", *J. Electrochem Soc*, vol 167, 110518 (2020)
- 10) J. Inamoto, et al : "Insight into the Origin of Rapid Charging Ability of Graphene-Like Graphite as a Lithium-Ion Battery Anode Material Using Electrochemical Impedance Spectroscopy", *J. Phys. Chem., C*, vol 126, pp. 16100-16108 (2022)
- 11) J. Inamoto, et al : "Synthesis of a flexible self-standing graphene-like graphite thin film and its application to an anode material for a thin-film all-solid-state lithium-ion battery", *Carbon Reports*, vol 1, pp. 142-146 (2022)
- 12) Y. Matsuo, et al : "Pyrolytic carbon from graphite oxide as a negative electrode of sodium ion battery, *Journal of Power Sources*", vol. 263, pp. 158-162 (2014)
- 13) Y. Matsuo, et al : "Electrochemical intercalation of sodium ions into thermally reduced graphite oxide", *Electrochemistry*, vol 83, pp. 345-347 (2015)
- 14) J. Inamoto, et al : "Graphene-like graphite as a novel cathode material with a large capacity and moderate operating potential for dual carbon batteries", *J. Inamoto, K. Sekito, N. Kobayashi, Y. Matsuo, J. Electrochem. Soc.* Vol 168, 010528 (2021)
- 15) Y. Matsuo, et al : "Factors Affecting the Electrochemical Behaviors of Graphene-Like Graphite as a Positive Electrode of a Dual-Ion Battery" *ChemSusChem*, e202201127 (2023)
- 16) J. Inamoto, et al : "Promise of dual carbon batteries with graphene-like graphite as both electrodes", *Carbon*, vol 216, 118512 (2024)
- 17) A. Inoo, et al : "Electrochemical Introduction/Extraction of Fluoride Ion into/from Graphene-Like Graphite for Positive Electrode Materials of Fluoride Shuttle Batteries" *ACS Appl. Mater. Interfaces*, vol 14, pp. 56678-56684 (2022)
- 18) F. P. McCullough, et al : "Secondary battery", US Patent 4830938, 1989.
- 19) P. Francis, et al : "Secondary electrical energy storage device and electrode therefor", US Patent 4865931, (1989)
- 20) J. A. Read : "In-Situ Studies on the Electrochemical Intercalation of Hexafluorophosphate Anion in Graphite with Selective Cointercalation of Solvent" *J. Phys. Chem. C*, vol 119, pp. 8438-8446 (2015)
- 21) J. Inamoto, et al : "Elucidating the Origin of the Low Anion Intercalation Potential of Graphene-like Graphite : A DFT Study" *J. Phys. Chem. C*, vol 127, pp. 9481-9488 (2023)

# Analysis of operational data of LL batteries at wind power plants by using exploratory data analysis and other analyses for their life prediction

Kei Hasegawa Daisuke Hosaka

Toshio Shibahara Noriyuki Tamura

Advanced Technology Research and Development Center, Business Strategy Sector

## 1 Abstract

Our "LL1500-W series" VRLA (valve regulated lead acid) battery was developed for load leveling in wind power plants. These batteries have been widely used in many plants, and their operational data have been accumulated since 2010. Battery life prediction by analysing the data is one of the main technologies to manage our "energy storage solution business". Data analysis using AI, which have been developing rapidly in recent years, is essential for the technology. In this study, we analyzed the operational data of the LL1500-W's large-scale energy storage system by using exploratory data analysis and other analyses to obtain information about the battery life prediction and factors affecting the battery life.

## 2 Features of technology

- Established a method for extracting factors that affect battery life by predicting battery life based on operational and inspection data from energy storage systems operating at nine wind power plants.
- Utilized exploratory data analysis with several machine learning methods.
- Real-time acquisition of battery degradation status can be deployed in energy storage services that simultaneously satisfy the user's needs for the operation of the energy storage system and the preservation of battery life.

## 3 History of development

We are transitioning to an "energy storage solution business," which aims to increase added value for customers by evolving conventional storage battery manufacturing and sales and incorporating new insights into storage batteries<sup>1)</sup>. We have initiated services such as traction battery status monitoring and renewable energy storage battery systems<sup>2)</sup>. Utilizing real-world data is a foundational technology for the energy storage solution business.

Since the VRLA battery "LL1500-W" was adopted to mitigate fluctuation in large-scale wind power plants in 2009, it has been operated at multiple client locations. Currently, to assess battery status in actual usage environments we are developing operational proposals to streamline life prediction and maintenance, and extend the lifespan of these batteries, by analyzing operational data with client permission.

Adapting to digital transformation (DX) is crucial as AI technology advances and societal systems evolve. The concept of "democratization of AI," which allows everyone to access advanced technology without specialized knowledge, including programming, is gaining recognition<sup>3)</sup>. We are also collecting data during various operations to begin utilizing these technologies.

The "exploratory data analysis (EDA)"<sup>4)</sup> that discovers various potential relationships between variables by visually analyzing a wide variety of data can be seen as the first step in developing an "energy storage solution business" that adds new insights to storage batteries. Implementing EDA effectively requires both knowledge of storage batteries and their usage, as well as data analysis techniques based on statistics and AI. The benefits of the "democratization of AI," where advanced technology is accessible without specialized knowledge, are particularly significant. We have introduced a statistical analysis tool, JMP<sup>®4)</sup>,

which is well-suited for EDA. This tool allows for various statistical and AI analyses without the need for coding and enables visual comparison of multiple analysis results, promoting company-wide data utilization as a key measure for DX.

This report presents the knowledge gained about predicting battery life and identifying factors that affect it. By performing analyses, including EDA, on operational data from batteries that had shorter lifespans than expected during periodic inspections of the LL1500-W installed at multiple wind power plants, we extracted the causes of degradation. This analysis was combined with operational data shared by clients.

## 4 Technical content

The analysis focused on data from nine wind power plants where the LL1500-W (WS, G) batteries were introduced, as shown in **Table 1**. This data includes standby voltage data for individual batteries and minute-by-minute operational data for each PCS, which controls each assembled battery (configured as 192 series x 2 parallel or 288 series x 2 parallel, with batteries installed in four tiers as shown in **Figure 1**). This data was obtained during periodic inspections, conducted once or a few times a year.

Table 1. Specifications of batteries to be evaluated

Client	(1) - (3)	(4) - (7)	(7) - (9)	
Battery specifications	LL1500-W		LL1500-WS(+G)	
Number of series x parallels	288x2	192x2 or 288x2	288x2	
Number of PCS's	2 - 6	5 - 14	12	12(+1)
Number of batteries	1,152 - 3,456	1,920 - 8,064	6,912 - 7,488	
Year of operation start	2010 - 2011	2015 - 2018	2018 - 2019	
Operating conditions	Battery voltage	1.8 V - 2.42 V		
	Battery current (charge)	225 A		300 A
	Battery current (discharge)	600 - 750 A		

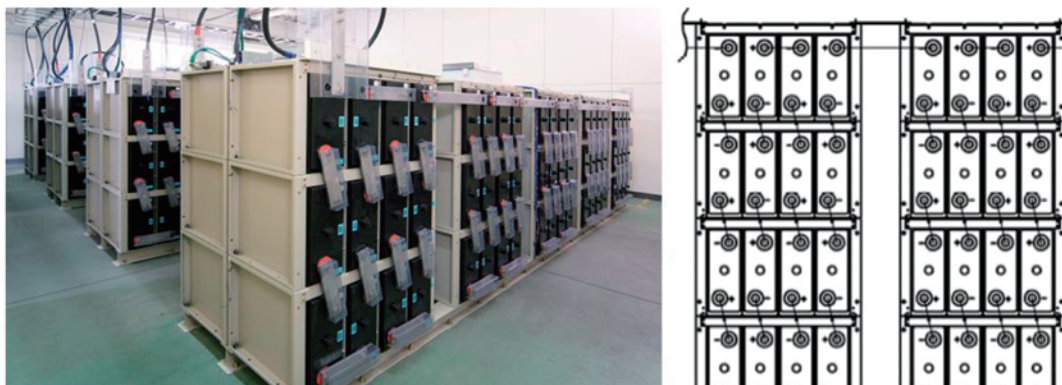


Figure 1. Exterior photo of assembled battery and installation diagram (logomark was deleted when the company was renamed)

During the periodical inspection, batteries whose average voltage is below a certain level within a PCS are considered degraded and replaced. To extract analysis targets for predicting battery life from the inspection data, we classified the monthly trends in the relative voltage of each battery. We then analyzed the trends for both normal and degraded batteries using "hierarchical clustering\*\*," a common machine learning classification method. **Figure 2 (left)** shows the classification results of all batteries at one client. The results are presented as a tree diagram with individual batteries at the right end. The more similar the trends, the closer they merge on the right side of the dendrogram. Pre-marked degraded batteries (light blue) and batteries replaced within the period (pink) were classified into the same group, successfully showing the tendency of voltage changes. **Figure 2 (middle)** displays part of the inspection results for each group (the four colors on the right side of the tree diagram correspond to the four colors in the center graph). We observed that the voltage of degraded batteries began to drop rapidly about six months before they were identified as degraded. There were also several batteries showing similar trends to these degraded ones. This indicates that battery life can be predicted by classifying and analyzing aging changes in battery voltage. Furthermore, analyzing only degraded batteries requires a sufficient number to obtain statistically reliable results, which is challenging for advance prediction.

However, including batteries with similar trends allows for predicting degradation trends before the number of degraded batteries increases. This makes it possible to predict and respond to rapid degradation in advance through appropriate battery monitoring equipment and data analysis.

We also found that the relative voltage of normal batteries was maintained for a long period (red and green) and that the vertical position of the stack affected voltage transition, as shown in **Figure 2 (right)**. This suggests that the installation environment could be a factor influencing battery life.

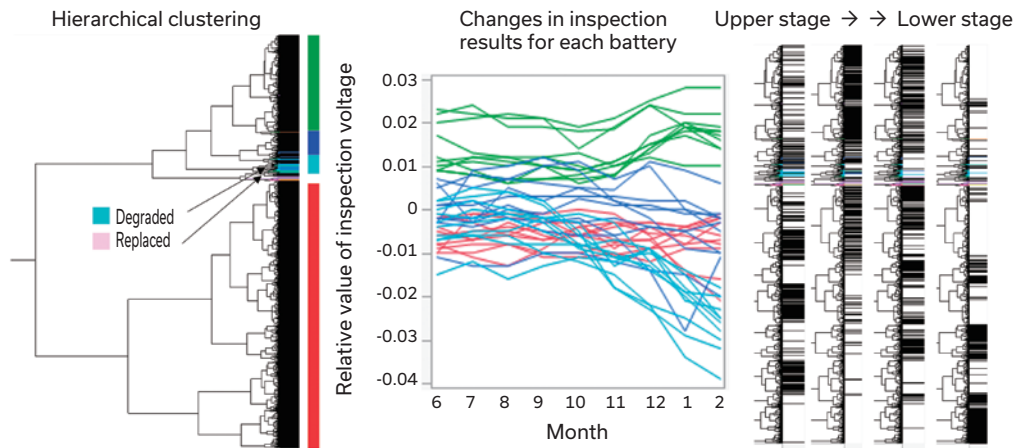


Figure 2. (Left) Classification result depending on "hierarchical clustering" of battery inspection data  
 (Middle) Changes in relative voltage (colors correspond to the bands shown in the left figure) of classified batteries (partial)  
 (Right) Differences in trends depending on battery stacking position for the classification result

Conversely, as shown by the PCS operating data in **Figure 3 (left)**, wind turbine operation involves repeated random charging/discharging and resting, focusing on a state of charge (SOC) around 70% (with full charge as 100%). For battery maintenance, equal charging is performed every two weeks to fully charge all batteries, keeping the voltage constant at around 2.5V. To extract from the operational data elements that are highly related to degradation, we performed a multiple regression analysis. We divided the operational data into "charge," "discharge," "stop," and "equal charge," and set the target variable to voltage and the explanatory variables to current, SOC, and temperature for charge and discharge. As an example, **Figure 3 (right)** shows the Effect Leverage plot\*\*\*, which isolates the effect of current versus voltage (each point represents one minute) and illustrates the relationship between voltage and current for discharging and charging based on monthly data from a particular customer. For both charging and discharging, most of the points are distributed along the same straight line. However, for charging, some high points deviate from this line. Comparing the frequency of these deviation points with the periodic inspection results revealed a high correlation with battery degradation at different rates at some customer locations. This suggests that by analyzing PCS operating data in real time throughout the year, we can predict battery life. In addition, we can suppress battery degradation by properly operating the PCS according to the specific conditions of each customer.

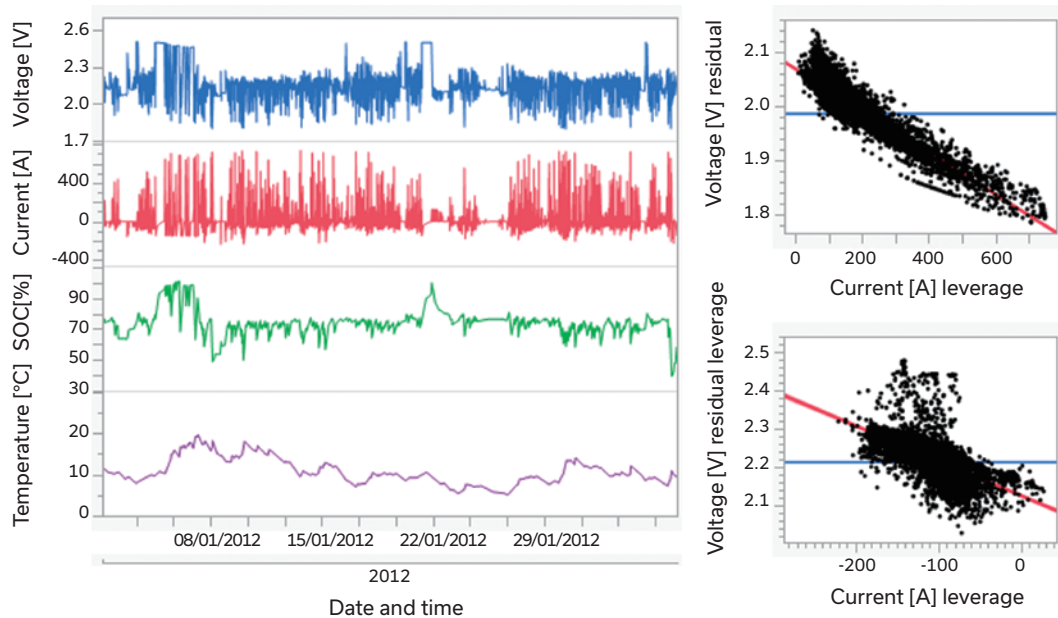


Figure 3. (Left) One month of operational data for a certain client, (Right) Effect leverage plot of current-voltage based on the multiple regression setting current, SOC and temperature as variables for each battery voltage during charging and discharging

## 5 Future developments

We found that we could predict battery life by analyzing changes in battery voltage over time through classification by EDA utilizing machine learning and multiple linear regression analysis of periodical inspection data and time series data in PCS units. This allowed us to establish a method for extracting factors affecting battery life, such as the installation environment. Utilizing these analysis methods can provide the degradation status of the system in real time. This approach can be expanded into an energy storage service that satisfies users' energy storage needs while preserving battery life.

### [Notes]

- \* Exploratory data analysis (EDA, Exploratory Data Analysis): Method of understanding overall data characteristics and potential relationships between data using data summarization and visualization techniques, which is mainly used to determine the direction of analysis before implementing more advanced analysis utilizing statistics and machine learning methods
- \*\* Clustering: Method for automatically classifying data through machine learning, which defines similarity between data for lots of data with the same format (images and graphs, etc.) to classify all data into several clusters by treating data with high similarity as a single cluster
- \*\*\* Effect leverage plot: Method of visualizing the effect of each explanatory variable on the target variable individually in multiple regression analysis, extract one explanatory variable (horizontal axis) and fixes the values of other explanatory variables to plot the relationship with target variable (vertical axis) as a figure

### [Reference]

- 1) Shoichi Hirota: Fundamental technology that supports our main products – toward a shift to energy storage solution business Energywith Technical Report No. 1, P. 6 (2023)
- 2) Website of Energywith Co., Ltd. "NEWS" <https://www.energy-with.com/news/>
- 3) Ministry of Internal Affairs and Communications "WHITE PAPER Information and Communications in Japan Year 2019" <https://www.soumu.go.jp/johotsusintokei/whitepaper/r01.html>
- 4) Website of JMP [https://www.jmp.com/ja\\_jp/home.html](https://www.jmp.com/ja_jp/home.html)

# Development of algorithm for image inspection of COS (Cast On Strap) process

Masahide Ohno

Automotive Battery Business Headquarters, Saitama Works Production Engineering Dept.

## 1 Abstract

A short-circuit failure of an automobile battery is a fatal defect resulting in malfunction of the battery. The short circuit failure is occurred in the COS process, and molten lead is crossed between the positive and negative plates, this is causing a short circuit. Currently, defects are detected by visual inspection by workers, but it's desired to introduce image inspection to automate inspections and improve quality. Although the introduction of image inspection has been considered in the past, it has not progressed due to the fact that defects could not be imaged accurately. In this research, we examined to get proper imaging environment and the judgment algorithm. After that, this image inspection has introduced in the mass production.

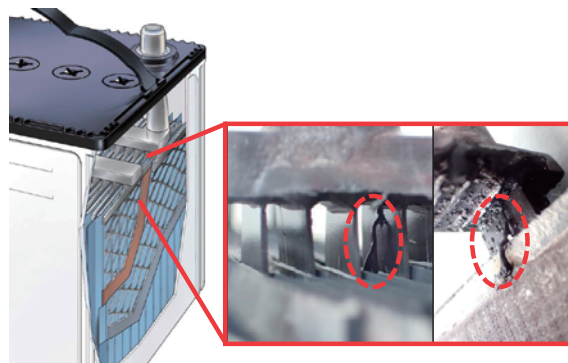


Figure 1. Example of applicable defect

## 2 Features of technology

- Achieving 100% reliable inspection and prevention of defect leakage by introducing image inspection
- Enabling the creation of a database or application to identify the causes of defects, as inspection data can now be digitized

## 3 History of development

Lead acid batteries are widely used for car engine starts and auxiliary equipment. In the manufacturing process of lead acid batteries, the COS (Cast On Strap) process is critical. During the soaking of the COS accumulation part, lead can spatter and spread between the positive and negative electrodes, causing a short circuit that leads to functional failure. Currently, workers perform visual inspections of the external appearance, but this method has several issues: (1) the inspection points and defects are very small and difficult to detect, (2) the process places a heavy burden on workers, and (3) it is not possible to create a database or record images.

To address these problems, automate the inspection process, improve quality, and identify defect causes through digitalization,

we have been considering a shift to image inspection. Although we have considered this in the past, we did not introduce image inspection due to the difficulty in photographing the defects themselves. The defects vary in size, shape, and occurrence location, making it challenging to create a defect judgment logic. This report summarizes the results of our examination of the imaging method and logic for detecting these defects.

## 4 Technical content

A major prerequisite for introducing image inspection is the ability to accurately capture images of defects. **Figure 2** compares the imaging capabilities of the reflected light imaging method and the waveform conversion sheet method. In the reflected light method, defects from the middle to the back side cannot be imaged accurately. However, the waveform conversion sheet method accurately captures the shape of these defects. The combination of the waveform conversion sheet and a blue cut filter has enabled imaging similar to transmitted light (shadow pictures).

		Imaging method		
		External view	Reflected light method	Waveform conversion sheet method
Location of defect	Front side			
	Near the middle			
	Back side			

Figure 2. Comparison of imaging between reflected light imaging method and waveform conversion sheet method

To comprehend the shape of the defects, we performed imaging on the mass production line. An excerpt is shown in **Figure 3**. We confirmed that the shape, size, and occurrence location of the defects were random. Moreover, we verified that it is possible to image even very small defects. To conduct desk-based judgment logic verification, we used images of both non-defective and defective items to create a simple model.

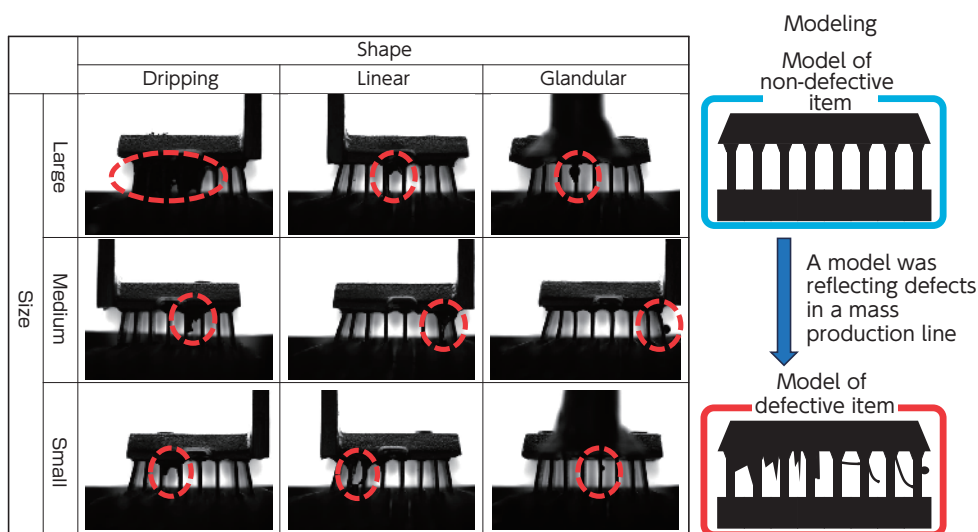


Figure 3. Defect shooting result in mass production line

The installation of the judgment window is shown in **Figure 4**. For image inspection, the judgment is based on a threshold value applied to a captured image using tools that measure distance and area. The judgment window refers to the area to which these tools are applied and is also known as the inspection range.

For this inspection, we adopted the installation of multiple rows of judgment windows spanning the entire horizontal length. This approach accommodates variations in the shape and range of non-defective items, ensuring that the inspection can account for these variations.

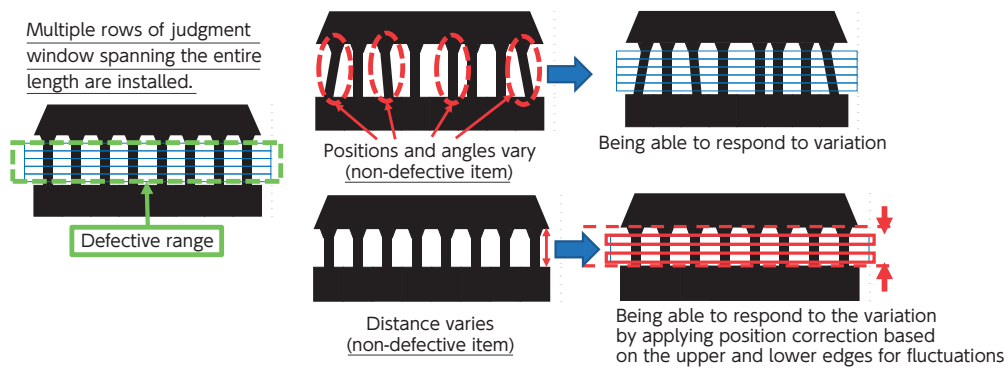


Figure 4. Examining the installation of judgment window

As a result of examining judgment logic, it was possible to identify defective patterns using three tools shown in **Figure 5**. We considered using multiple tools to determine the same defective location as much as possible to improve certainty and reliability of judgment.

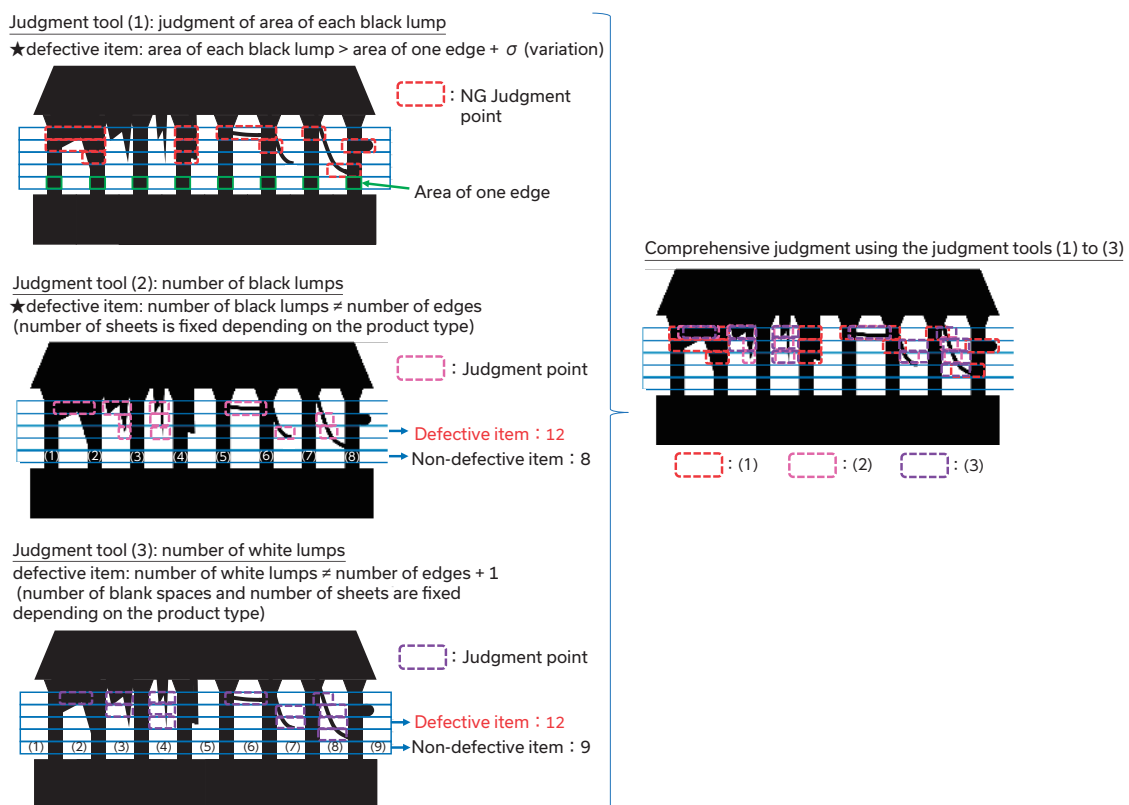


Figure 5. Judgment logic

## 5 Future developments

- Expanding the inspection to all lines
- Defect statistics through automation of sorting NG images using machine learning and making database of inspection result
- Identification of cause of defect by analyzing the database

# A new DIN-Type Traction Battery

Warakorn Suriyatun Pratan Pongphongpoon  
Chakkapan Sangkaew Muneyoshi Noda  
Research and Development Section Engineering Department  
Thai Energy Storage Technology PLC.

## 1 Abstract

"The term 'batteries' describes battery-powered traction power supplies, also known as traction batteries, which are broadly classified into two types. The first type, defined by JIS standards or BS (British Standards), are called 'narrow cell' with a width of 160 mm or less. The second type, defined by DIN standards set by the German Institute for Standardization, are called 'wide cell' with a width of 198 mm or less."

Note that the terms "narrow-cell" and "wide- cell" are not interchangeable due to significant differences in width dimensions. A global overview reveals that about half the battery types mentioned are in use worldwide.

The market for these batteries is split nearly evenly between the two types and development and expansion of the product line are crucial to boost market share. Moreover, technologies developed under the JIS standard, e.g. for glass tubes, have also been adapted for use in DIN standard products.

## 2 Features of technology

- Optimal material specification.
  - ① Optimized positive active material
  - ② Adopt a glass tube, with generally excellent durability at high temperature
  - ③ A separator for high charge acceptance
- Privileged charging specification for protect stratification defect.

## 3 Technical Content

- (1) Development terms are examined through benchmarking and design reviews, which incorporate failure mode analysis(**Figure 1**). This analysis particularly considers the implications of shape changes from JIS standards on battery performance. The review identified potential issues such as low capacity, low charge acceptance, and reduced lifespan, which stem from increased resistance caused by changes in battery height. To address these issues, adjustments were made to the active material, glass tube, separator, and charging conditions.

FUNCTION	Potential Failure	Control prevention	Requirement
Higher than JIS	Low Capacity	①Bulk ②Tube ③Charge	→ High efficiency → Low resistance → Suitable energy
	Low Charge acceptance	→ ④Separator	→ Low resistance → Aided to prevent acid stratification
	Short life	→ ⑤Recovery charging → Bulk density	→ Suitable charging method → High efficiency

Figure1. Failure mode effect analysis in the development of a DIN Type Traction battery

(2) Optimized positive active material

The positive active material is a crucial factor that influences both the capacity and durability of batteries. In this development, the density of the active materials has been optimized to enhance these characteristics. Additionally, the formation production conditions have been thoroughly studied to ensure efficient formation of PbO<sub>2</sub>, further improving the battery's performance and longevity.

(3) Adopt a glass tube

Glass tubing exhibits excellent durability characteristics under high temperatures. Furthermore, several materials have been examined for their high-rate discharge characteristics to enhance overall performance.

(4) Low-resistance separator

The PE separator has been optimized to achieve minimize electrical resistance, which is crucial for efficient battery performance. The resistance of the PE separator is influenced by its porosity and electron transfer characteristics. In this development, several materials were evaluated for their charge acceptance characteristics. Improved charge acceptance limits any increase in voltage, which helps the battery function more efficiently. The separator chosen for this application effectively suppresses any increase in voltage.

(5) Privileged charging specification for protect stratification defect

Battery durability is critically dependent on its ability to fully recover after heavy usage, specifically after discharging 75% of its capacity. To address this, new charging patterns were explored, including daily charging for regular recovery and weekly "configuration charging" for comprehensive maintenance. A new charging method was developed that prevents stratification through gassing, thereby enhancing the battery's durability.

## 4 Product Specification

**Table 1** shows the specifications of battery models launched in 2022. In the first phase, there are a total of nine models, covering a range of battery capacities from 345 Ah to 930 Ah, each at 2 Volts per cell. These 2V cells can be assembled into various configurations ranging from 24V to 80V per set. An example of a 2V cell assembled into a 48V battery set is illustrated in **Figure 2**. Additionally, the discharge characteristics of 4PZH620 model are detailed in **Figure 3**.

Table 1. DIN Type Traction Battery Specification (Step 2)

List	Battery Model								
	3PZE345	4PZE460	3PZH465	4PZG560	5PZE575	4PZH620	5PZG700	5PZH775	6PZH930
Capacity At 5 Hour rate (AH)	345	460	465	560	575	620	700	775	930
Total plate number	7	9	7	9	11	9	11	11	13
Plate size	E	E	H	G	E	H	G	H	H
• Width (mm)	65	83	65	83	101	83	101	101	119
• Length (mm)	198	198	198	198	198	198	198	198	198
• Height (mm)	545	545	720	685	545	720	685	720	720
• T-Height (mm)	576	576	751	716	576	751	716	751	751
Battery Weight W/ Acid (Kg.)	21	28	28	34	33	36	41	44	52
Electrolyte Volume (Liter)	4	5	5	6	6	6	7	8	9



Figure2. DIN Type Traction Battery new model (2V Single cell) and battery set (48V Cells).

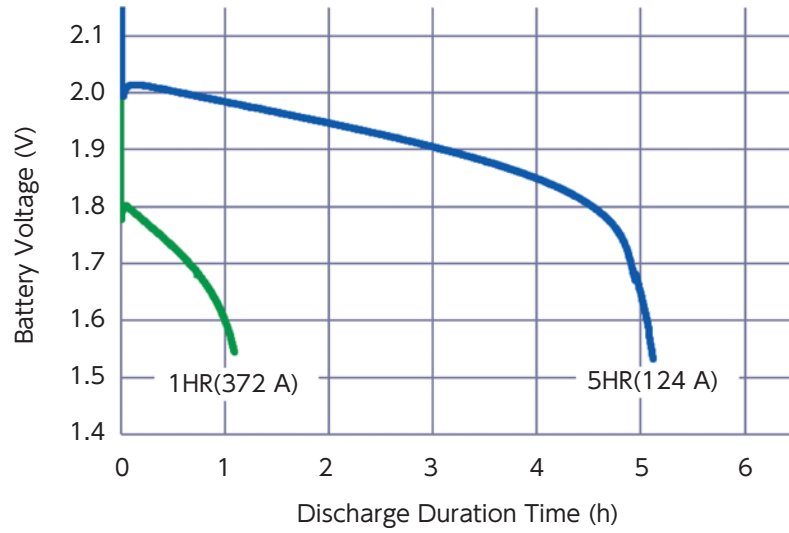


Figure3. Discharge Characteristics (4PZH620)

## 5 Next step

- Material Evaluation: Consider selecting high-quality materials to enhance product quality and increase profitability.
- Battery Development: Develop new battery models with two capacity ranges: from 230 to 310 Ah and from 980 to 1240 Ah.

## 6 Acknowledgment

- This work was supported by EW, Industrial Battery R&D Dept.

# "withBMS", the battery monitoring service of lead acid batteries for electric forklifts

Akihiko Kudou Koji Hayata

New Business Development Sector,  
Monitoring System Business Promotion Group

## 1 Abstract

We developed "withBMS", the battery monitoring service of lead acid batteries for electric forklifts. Battery Monitoring Unit (BMU) measures battery operating data including electrical current, total voltage, ambient temperature, and electrolyte level automatically. IoT gateway transfers the measured battery operation data from BMU to the battery monitoring service platform. Based on the stored battery operating data, the service platform creates the battery alert and some reports as needed and provides it.

## 2 Features of technology

- Development of BMU with high measurement accuracy to withstand harsh operating environments of electric forklift and remain reliable
- Development of a numerical index to pinpoint the battery degradation status based on the battery measurement data

## 3 History of development

The mainstream batteries installed in electric forklifts are lead acid batteries, which are expected to continue being used due to their excellent recyclability. Forklifts frequently discharge large amounts of power during transportation and lifting heavy objects, characterized by significant load fluctuations. This makes it challenging to numerically detect battery degradation.

Currently, the degradation status of a battery installed in a forklift is evaluated based on the measurement values of electrolyte specific gravity and cell voltage when the operation is stopped, along with visual inspections conducted periodically (monthly, annually) by inspectors. Although a discharge test using a charge-discharge control device can determine battery degradation, this method is not easily applicable to batteries in operation on forklifts. Therefore, it is desirable to assess battery degradation numerically based on measurement data from batteries in operation.

Maintenance work, such as water supply and equal charging, is required for liquid lead acid batteries. However, field workers, who often lack knowledge about batteries, are usually responsible for this work. Neglecting these tasks can lead to premature battery degradation and, in the worst case, an explosion. Hence, there is a demand for understanding the actual status of maintenance work and providing support for improvements.

Given this background, we have developed a battery status monitoring service for electric forklifts.

## 4 Technical content

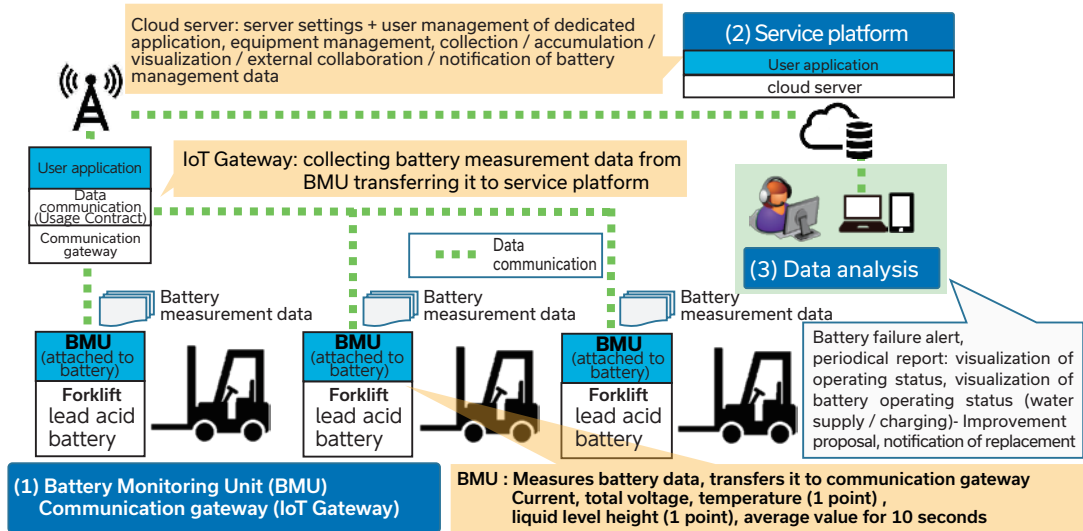


Figure 1. General configuration of battery monitoring service and service  
Transferring the battery measurement data from BMU to IoT Gateway and cloud server, providing the data analysis data as a service

The general system configuration is shown **Figure 1**. The Battery Monitoring Unit (BMU) attached to a lead acid battery for forklifts continuously measures the battery's current, total voltage, temperature, and liquid level height. This measurement data is then transferred to the communication gateway (IoT Gateway). The communication gateway sends the battery measurement data to the service platform. Based on the accumulated battery measurement data, the service platform generates battery failure alerts and periodic reports, providing these as a service.

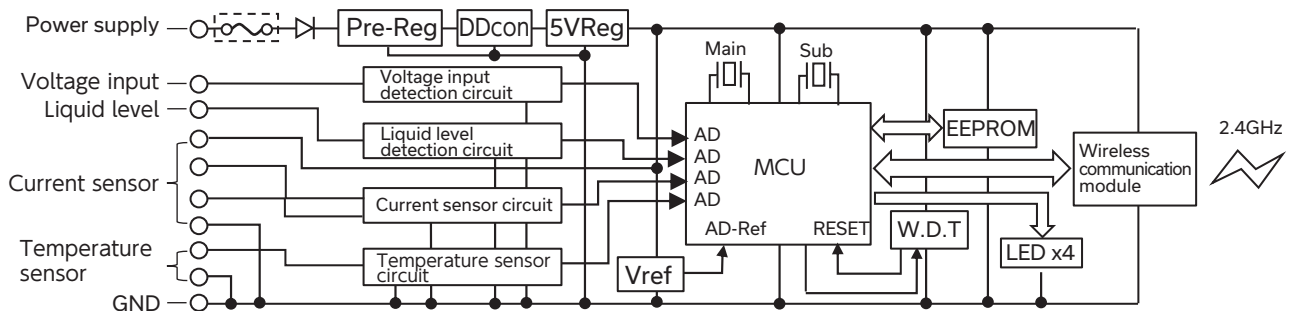


Figure 2. Internal configuration diagram of BMU

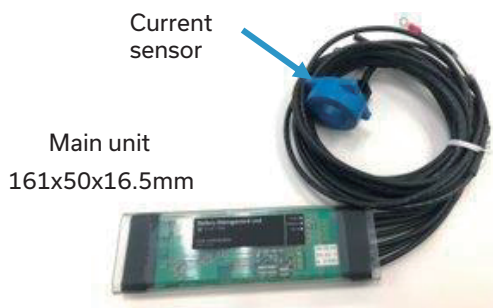


Figure 3. Battery Monitoring Unit (BMU)

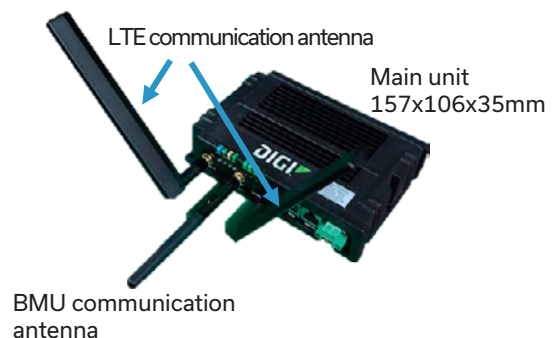


Figure 4. Communication gateway (IoT Gateway)

**Figures 2 to 4** show the internal configuration of the BMU and its external appearance, including the IoT Gateway, below. The BMU measures the battery's current, total voltage, temperature, and liquid level height, and transfers the average value over 10 seconds to the IoT Gateway through wireless communication. Since the BMU is attached to a forklift battery, it must be compact,

with high measurement accuracy, and reliability to withstand harsh environments. For this development, we applied the design standards and evaluation tests used for vehicle battery controllers. We also practically established<sup>1)</sup> a battery monitoring system for stationary lead acid batteries. The primary difference is that the degradation state of the battery in the stationary system is calculated by measuring the charging and discharging current. A hall-type current sensor is used, which can be easily attached to an electric forklift already in operation by simply passing the charge-discharge current line through the sensor.

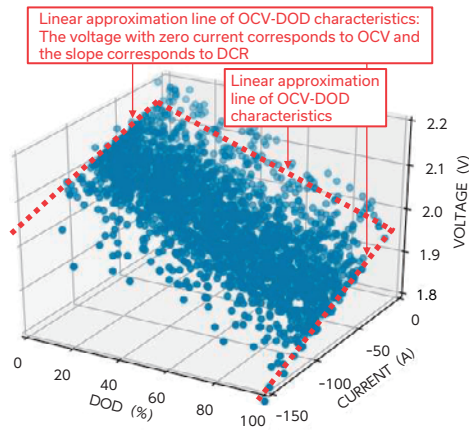


Figure 5. 3D plot of voltage - current - DOD (new battery)

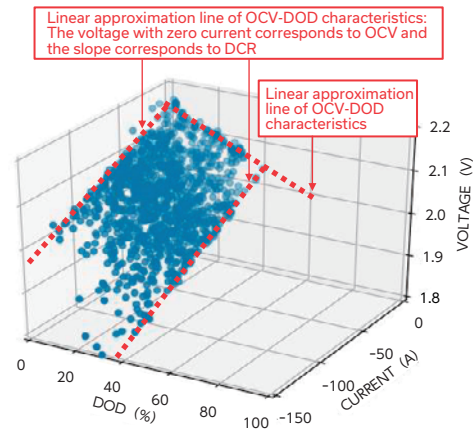


Figure 6. 3D plot of voltage - current - DOD (deteriorated battery)

**Figures 5 and 6** show the 3D plot indicating the current and Depth of Discharge (DOD) dependence of voltage during discharge. DOD 0% (SOC 100%) indicates the fully charged state, and DOD 100% (SOC 0%) indicates the state when the rated capacity is discharged. DOD (SOC) is calculated from the integrated value of discharge current after a full charge. As shown in the figures, the larger the discharge current and the higher the DOD, the lower the voltage. The slope differs between new and deteriorated batteries, and is steeper for deteriorated batteries. This demonstrates that the voltage drop relative to DOD and the voltage drop relative to current become more pronounced as the battery deteriorates.

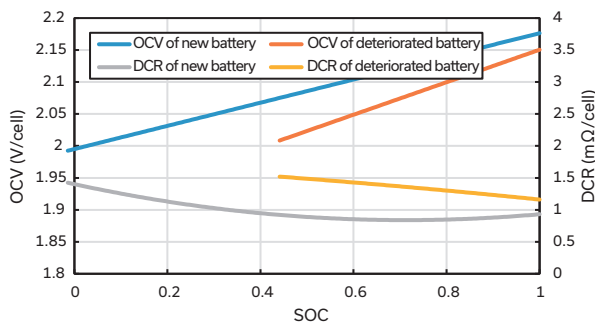


Figure 7. Example of SOC dependency of approximate OCV and DCR

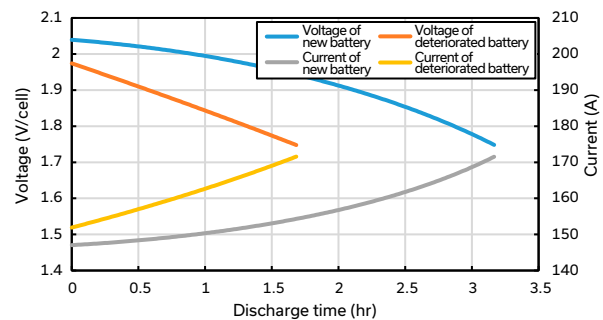


Figure 8. Example of estimated discharge characteristics at maximum power

**Figure 7** plots the SOC (DOD) dependency by first order approximating the I-V characteristics at each SOC (DOD) and setting the approximate value when the discharge current is 0A to OCV and setting the slope of I-V characteristics to DCR.

As shown in the figure, the decrease in OCV is greater for deteriorated battery than for new ones and DCR is larger for deteriorated batteries than new ones. This means that the deteriorated battery has a lower capacity and larger DCR.

Generally, capacity reduction ratio (SOH-Q) and internal resistance reduction ratio (SOH-R) are used as indicators to show the degradation status of the battery. In this figure, SOH-Q indicates the ratio of reciprocal of slope of OCV-SOC characteristics to new battery and SOH-R indicates the ratio of DCR to new at SOC50%.

**Figure 8** shows an example of calculating discharge characteristics at maximum discharge power from approximated OCV-SOC characteristics and DCR-SOC characteristics. For applications that require power such as forklift, the discharge duration at maximum discharge power is important. Thus, the ratio of this discharge duration time to new battery is set as a new indicator, SOH-P. The maximum discharge power is set as the maximum value in use using the maximum power value in operation.

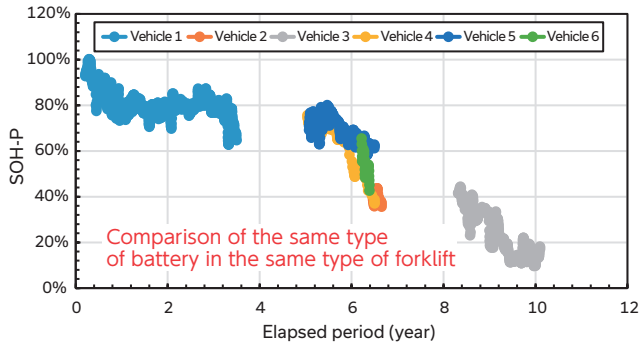


Figure 9. Example of transition of SOH-P

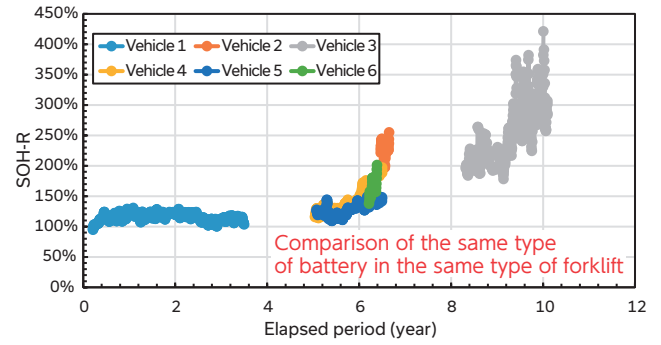


Figure 10. Example of transition of SOH-R

**Figures 9 and 10** show an example of the State of Health (SOH) transition during actual operation. This example illustrates batteries installed in six forklifts of the same model in the field. The horizontal axis represents the elapsed time since the battery manufacturing date. SOH-P decreased over the years, while SOH-R suddenly increased as battery degradation progressed, leading to the termination of operation.

Since the BMU continuously measures the battery data, it is possible to visualize the operational status of a vehicle using this data. Moreover, it enables the notification of battery failure alerts, visualization, and improvement proposals for battery operation status (such as water supply and charging). Additionally, it allows for the estimation of the remaining battery life based on the cumulative discharge amount and the battery design value, provided the battery has been monitored since it was new.

## 5 Future developments

- Improve accuracy of indicators for battery degradation

### [Reference]

- 1) Akihiko Kudo et al: Next-generation monitoring device (Gen2) Hitachi Chemical Technical Report, No. 60

Contact information

For any question relevant to the contents, please use the following contact form on our website :

**<https://www.energy-with.com/en/>**

---

**Energywith Technical Report No. 2 (May 2024)**

Energywith Co., Ltd.  
AKS building 8F, 3, Kandaneibeicho, Chiyoda Ward, Tokyo-to, 101-0022, Japan,  
TEL: +81-3-6811-6510 (main switchboard)  
Printed by Hitachi Document Solutions Co., Ltd

© 2024 Energywith Co., Ltd. All rights reserved. Printed in Japan (posting without permission prohibited)

---